

On chemical bonding of Helium with hcp-Beryllium

A. S. Bakai

National Science Centre Kharkiv Institute of Physics and Technology, 61108 Kharkiv, Ukraine

A.N. Timoshevskii* and B.Z. Yanchitsky

Institute of Magnetism, National Academy of Science Ukraine, 03142 Kiev, Ukraine

Chemical inertness is the key property of helium determining its solubility, distribution and accumulation kinetics in metals. Against all expectations, our *ab initio* calculations show a substantial chemical bonding between He and Be atoms in the hcp-Be matrix when He occupies a non-symmetric position in a basal plane.

PACS numbers: 61.72.jj, 71.55.Ak

Keywords: helium in hcp-beryllium, electronic structure, *ab initio* modeling

Helium is the most inert element of the periodic table. Having its first electronic level (1s-shell) completely occupied, the electro-neutral state of the atom is very stable. In an excited state, when one of the electrons moves to the next energy level, He may form short-living dimers with fluorine or chlorine: He-F and He-Cl. The very existence of these excimers can be viewed as a proof of the degree of chemical inertia of helium. Chemical inertia determines the helium behavior in the irradiated structural materials of nuclear reactors, where He is formed in substantial amounts due to nuclear fission reactions. Accumulation of He in metal alloys in the form of the inert lattice gas, leads to their so-called “helium swelling” and embrittlement.

We studied the distribution of interstitial He in hexagonal close-packed (hcp) beryllium by means of *ab initio* modeling. Employing a pseudopotential technique¹, we obtained a surprising result: interstitial He forms a chemical bonding with Be matrix².

Further, using a highly accurate all-electron full-potential linearized augmented plane wave (FLAPW) method, we confirmed results of pseudopotential calculations, analysed partial DOSes and their integral quantities. We performed analysis of chemical bonding in the Be-He system using Crystal Orbital Hamilton Population (COHP) indicator³, implemented in SIESTA package⁴. In this Letter the results of our investigations are presented.

The Density Functional Theory (DFT) was used in Generalized Gradient Approximation (GGA⁵), as implemented in the *Quantum-ESPRESSO* (QE) program package¹. The same GGA approximation was used for calculations using FLAPW method (Wien2k software package⁶).

We have chosen 22 positions of interstitial He in hcp-Be (space group 194, two Be atoms in the unit cell at positions (1/3,2/3,1/4), (2/3,1/3,3/4)) as starting geometry configurations for the calculations. These positions included the centers of octahedra and tetrahedra, as well as the midpoints between the centers of these polyhedra (Fig. 1). The midpoints between the two neighboring lattice sites were also included as testing positions for in-

terstitial He. All positions were generated by relation: $1/2(p_1, p_2, p_3) + 1/2 \sum_{ij} (\mathbf{r}_i + \mathbf{r}_j)$, where summation i, j is over octahedra and tetrahedra, and p_1, p_2, p_3 take values $\{0, 1\}$ independently.

Calculations were performed for Be₆₄He (4x4x2 hcp Be unit cells), Be₉₆He (4x4x3 hcp Be unit cells) supercells and included relaxation of atomic positions. Atomic nuclei were moved to their equilibrium positions while forces acting on nuclei were greater than 1 mRy/Bohr. Lattice parameters of supercells were according to hcp-Be, that were obtained by minimisation of the total energy with respect to a and c/a . Calculated lattice parameters from pseudopotential method $a = 2.246$ Å, $c/a = 1.573$ are comparable with experimental values $a = 2.2858$ Å, $c/a = 1.5687$, whereas FLAPW data $a = 2.272$ Å, $c/a = 1.565$ are in adequate agreement.

On the basis of the total-energy calculations, we found five equilibrium positions of He atom (zero force on He nucleus) in the beryllium lattice. Fig. 1 shows these equilibrium positions as green and orange circles. To denote positions we are using Wyckoff notations⁸ and fractional coordinates (Table I). The other 17 studied positions of He atom in hcp-Be matrix, including the tetrahedral one, were found to be non-equilibrium. Among 5 equilibrium positions, three positions (b), (d), (h_0) are stable (Fig. 1a, green circles), and two (a), (g) are unstable (saddle points with negative curvature of potential energy surface for He displacement along [0,0,1]; Fig. 1a, orange circles). Both FLAPW and pseudopotential methods produced close values of He-Be bond length (Table I). The energy of isolated helium atom, which is needed to calculate the solution energy of He in Be lattice, was obtained by performing total energy calculations for simple cubic lattice of He atoms with lattice parameter 10 Å. Calculated solution energies of interstitial He are presented in Table II. The previous *ab initio* results of Ganchenkova *et al.*⁹ and Zhang *et al.*^{10,11} are also shown for comparison.

According to all studies^{9–11} He solution energy is in the range of 5.5–6.5 eV. He solution energy for octahedral cavity (a) position has the value of 6.0–6.5 eV and is in good agreement with the value of 6.1 eV from^{10,11} and close to 6.8 eV reported by Cayphas¹² from EAM poten-

tial calculations. Solution energies for positions $(b), (d)$ are in well agreement between researches. According to our present findings, the most energy favorable He position is (h_0) with the solution energy of 5.3-5.8 eV. It was obtained by moving He from points $h(x = 1/2, z = 1/4)$ and $k(x = 1/2, z = 5/8)$ (Fig. 1a, grey circles). In (h_0) He is located in the basal plane near a strongly displaced Be atom (Fig. 1b). It is worth to be noted, that this position (h_0) was never considered in previous studies⁹⁻¹¹ as a place for He.

Zero point vibration energy (ZPE) is not small for interstitial He. To estimate this quantity we calculated phonon frequencies at Γ -point for Be_{96}He and hcp- Be_{96} supercells within DFPT approach as implemented in QE software package. ZPE was calculated as a sum of delta functions, that typically produces 5% uncertainty of exact value for supercells of such size (see e.g. ref. 13). For positions $(b), (d), (h_0)$ ZPE contributions to the solution energy are 0.09, 0.08 and 0.15 eV, that does not change energy landscape significantly. This correlates well with result by Zhang *et al.*¹⁰, where ZPE correction was found to be in narrow range of 0.12-0.13 eV for all studied positions.

A deep potential well for the (h_0) position, the presence of only one Be atom in the first coordination shell of He and small He-Be distance (1.29 Å) for this configuration demonstrate the existence of chemical bonding between He and Be atoms. To get further insight and investigate the nature of this bonding, we proceeded with the highly-accurate FLAPW method to calculate the density of electronic states (DOS).

Two configurations of He in Be matrix were chosen for comparative DOS analysis, (a) and (h_0) (Fig. 1). Figures 2b and 2c show partial DOSs of the He-Be system for the cases, where He occupies the octahedral cavity (a) and the position in the basal plane near the lattice site (h_0) . Partial DOSs for the pure hcp-Be system are also shown in Fig. 2a for comparison. It is seen that the valence band of He-Be system is formed by the He 2s

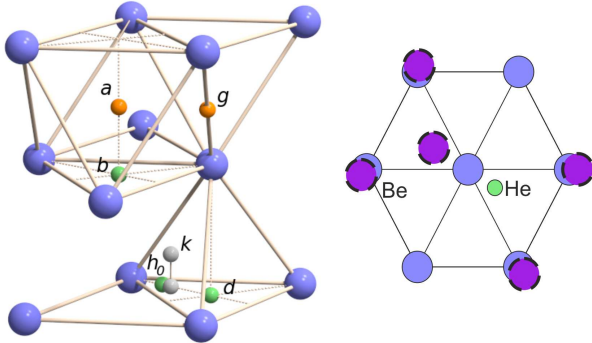


FIG. 1. (Color online) Equilibrium positions of He in hcp-Be and atomic relaxation near He atom in position (h_0) . Stable positions (b, d, h_0) are shown as green circles, unstable (a, g) as orange ones.

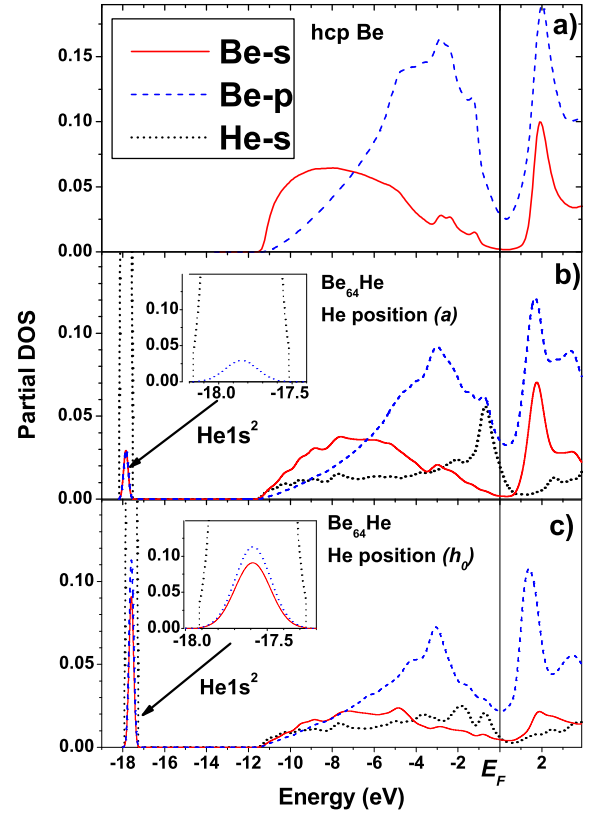


FIG. 2. (Color online) Partial DOSes of the He-Be system: a) pure hcp-Be; b) He occupies the octahedral cavity (a) ; c) He at position (h_0) .

and the Be 2s- and 2p-states. The occupied He 1s-state is located 18 eV below the Fermi level. The densities of electronic states for He in one of the (a) or (h_0) positions appear to be substantially different, which reflects the different degree of overlap of He electronic charge with that of neighboring Be atoms.

Together with substantial decrease of the He-Be distance, the (h_0) configuration shows the increase of hybridisation of the He s-states with the 2s- and 2p-states of Be. The hybridisation of low-lying He 1s-state and 2p-states of Be also takes place. We need to mention here

TABLE I. Equilibrium positions of He atom in hcp-Be (space group 194), number of nearest Be atoms z , distance He-Be d (Å), calculated by plane-wave pseudopotential (PS, QE) and FLAPW (Wien2k) methods for Be_{64}He , Be_{96}He structures.

Position	Wyckoff notation	z	PS		FLAPW	
			64 d	96 d	64 d	
(0, 0, 0)	2 a	unst.	6	1.794	1.791	1.803
(0, 1/2, 0)	6 g	unst.	2	1.512	1.512	1.505
(0, 0, 1/4)	2 b	stb.	3	1.564	1.564	1.571
(2/3, 1/3, 1/4)	2 d	stb.	3	1.726	1.719	1.740
(0.465, 0.930, 1/4)	6 h ₀ ^a	stb.	1	1.287	1.290	1.266

^a subscript "0" indicates minimal solution energy among all positions

TABLE II. Solution energies of helium (eV) in hcp-Be from DFT(GGA) calculations. VASP – Vienna *Ab initio* Simulation Package^{16,17}; “Y/N” symbols indicate the presence or absence of ZPE contribution.

Source	Method	ZPE	Cell	He position				
				(a)	(g)	(b)	(d)	(h ₀)
Present study	QE ^a	N	64	6.43	6.31	6.12	6.02	5.72
	QE	N	96	6.31	6.18	5.96	5.83	5.59
	QE	Y		unst.	unst.	6.05	5.91	5.74
	Wien2k ^a	N	64	6.06	5.91	5.72	5.78	5.34
Ref. 9	VASP ^b	N	96	unst.	unst.	5.81	5.82	×
Refs. 11,10	VASP ^b	Y	96	6.05	5.95	5.71	5.62	×

^a With PBE⁵ exchange-correlation.

^b With PW91^{14,15} exchange-correlation.

that the valence He *s*-states originate from the empty $2s^0$ atomic level of helium. When the Be-He system is formed, this empty state moves below the Fermi level, and becomes partially occupied, forming the *s*-band of Be-He system. These results reveal an increasing hybridisation of the He electronic states with those of neighbouring Be atom when helium is placed in (*h*₀) position. Due to the formation of the chemical Be-He bond, when the He atom is located in the stable equilibrium (*h*₀) position, attraction occurs between He and the nearest Be atom. As a result, the He and Be atoms are displaced from the centers of local symmetry and the distance between them is substantially reduced. The strength of the chemical bond is nearly equal to the total energy difference between (*a*) and (*h*₀) configurations, $\epsilon_{chem} \approx \epsilon_a - \epsilon_{h_0} \approx 0.7\text{eV}$.

The analysis of the partial density of states is not enough for complete understanding of the nature of the chemical bonding between He atom and Be matrix. We performed additional analysis of the chemical bond formation using the concept of bonding and antibonding states within the framework of COHP chemical bond indicator³. We used pseudopotential method and local atomic orbital basis set, as realized in SIESTA program package⁴. The calculations were done in GGA approximation for exchange-correlation functional⁵, and double-zeta polarized basis set was used, which included doubled $2s$ and $2p$ orbitals plus polarizing $3d$ orbital for Be atom, and doubled $1s$ plus polarizing $2p$ orbital for He. An optimization of atomic positions of Be₉₆He supercell with He in positions (*a*) or (*h*₀) was performed. The obtained relaxed positions of Be and He atoms were very close to those, obtained by the FLAPW and pseudopotential (QE) methods. The calculated Be-He bond lengths for positions (*a*), (*b*), (*h*₀) were 1.809 Å, 1.580 Å, 1.276 Å, which agrees well with the results, obtained by other methods (Table I).

We plot in Figure 3 the calculated COHP curves for He and Be atoms for He at positions (*a*), (*b*) and (*h*₀). Figure 3a) shows COHP curves for He atom and nearest beryllium Be_{He}. The plot demonstrates that only bonding states are present for He atom located in (*h*₀) position, which is not the case when He is located in (*a*)

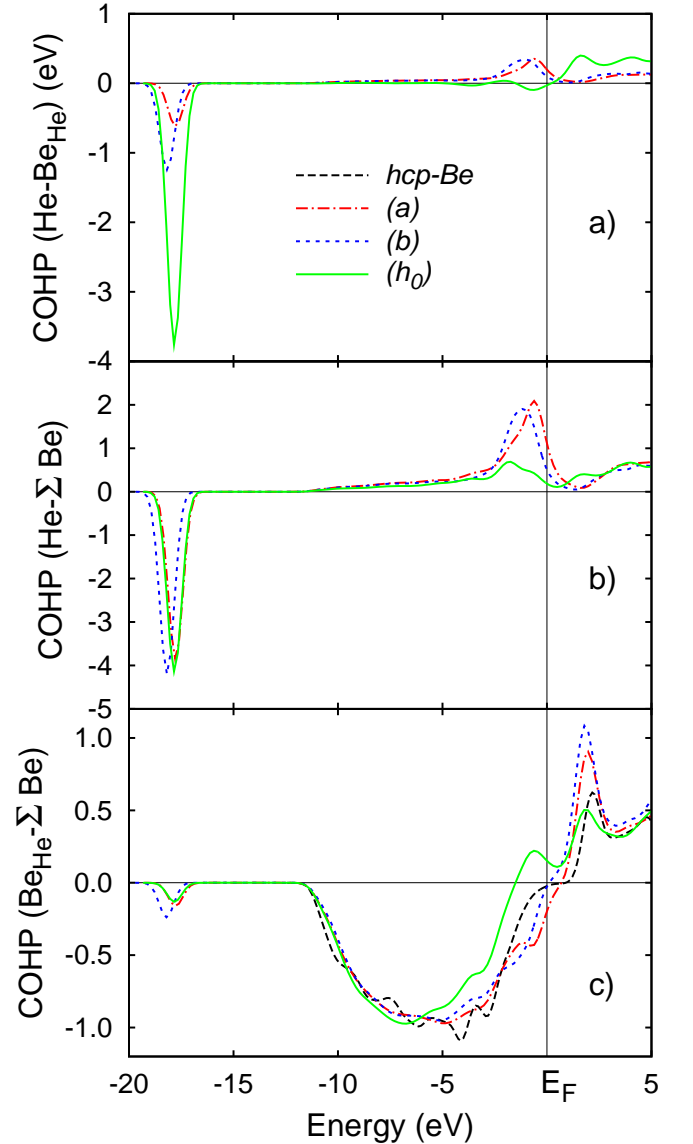


FIG. 3. (Color online) COHP curves for Be₉₆He structure with helium at positions (*a*), (*b*) and (*h*₀): a) He and nearest Be_{He}; b) He and beryllium matrix; c) Be_{He} and beryllium matrix

and (*b*). Antibonding states near Fermi level originate from atomic He $2s$ -states (see Fig. 2b). Integrated values (to Fermi level) of these COHP curves for (*a*), (*b*), (*h*₀) positions are 0.32, -0.19, -3.42 eV.

COHP curves for He and whole beryllium matrix are shown in Figure 3b. The bonding strength of He $1s$ -states is the same for all 3 positions, but reduction of He-Be_{He} distance (especially strong for (*h*₀)) decreases antibonding states near Fermi level. Integrated COHP values are 1.93, 1.38, -1.09 eV, confirming He-Be bonding in position (*h*₀). This fact, as well as the small He-Be_{He} interatomic distance, allows us to conclude that a distinct molecular He-Be_{He} pair is formed in Be-hcp matrix.

Soluted in hcp beryllium, helium also changes Be-Be

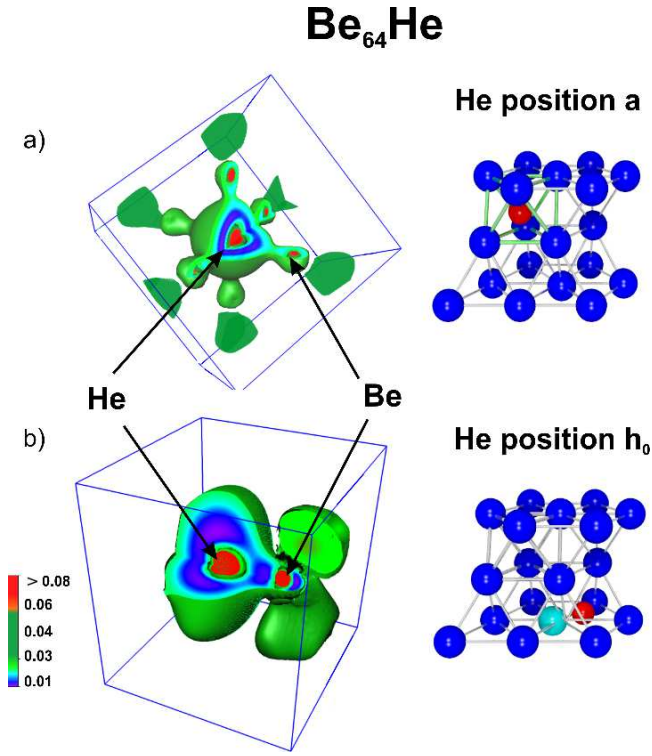


FIG. 4. (Color online) Distributions of electron density ($e/(a.u.)^3$) for structure $Be_{64}He$ with He atom: a) in position (a) and b) in position (h_0).

bonding. Figure 3c shows COHP curves for Be_{He} atom and beryllium matrix, as well as COHP curve for pure hcp-Be. It can be seen that the curves for (a), (b) positions are close to that of hcp-Be. For (h_0) position, He atom induces antibonding Be-Be states near Fermi level, thus weakening Be-Be bonding.

To visualize the chemical bond in Be-He system, we analyzed the spatial distribution of valence electronic density in model $Be_{64}He$ supercell, when He is located in (a) or (h_0) positions. Figure 4 shows these distributions for density values larger than $0.01 e/(a.u.)^3$. When He is located in the octahedral cavity (Fig.4a), we do not observe electronic charge concentration between He and Be atoms (marked as red and blue spheres respectively), and the electronic density (marked as a green cloud) appears to be "pushed" out of the Be octahedron. Completely different charge distribution is observed in case of He located in (h_0) position (Fig. 4b). In this case the electronic charge "connects" He and Be atoms, which shows a covalent character of chemical bonding.

In conclusion, our *ab initio* calculations show a substantial chemical bonding between He and Be atoms, when He occupies a non-symmetric position in a basal plane in the hcp-Be matrix. This fact should be taken into account, while analysing the kinetics of the process of helium accumulation in hcp-Be. The experimental evidence of the existence of the Be-He bond may be obtained by means of different methods, including the diffraction experiments. We believe that our results should stimulate the experimental efforts in this direction.

* Author to whom correspondence should be addressed. Electronic address: tim@imag.kiev.ua

¹ P. Giannozzi, S. Baroni, N. Bonini, M. Calandra, R. Car, C. Cavazzoni, D. Ceresoli, G. L. Chiarotti, M. Cococcioni, I. Dabo, et al., J. Phys.: Condens. Matter **21**, 5502 (2009).

² A. S. Bakai, A. N. Timoshevskii, B. Z. Yanchitsky, Low Temp. Phys., **37**, 992 (2011).

³ R. Dronskowski and P. Bloechl, J. Phys. Chem. **97**, 8617 (1993).

⁴ J. M. Soler, E. Artacho, J. D. Gale, A. García, J. Junquera, P. Ordejón, and D. Sánchez-Portal, J. Phys.: Condens. Matter **14**, 2745 (2002).

⁵ J. P. Perdew, K. Burke, and M. Ernzerhof, Phys. Rev. Lett. **77**, 3865 (1996).

⁶ P. Blaha, K. Schwarz, G. Madsen, D. Kvasnicka, and J. Luitz, *WIEN2k*, An Augmented Plane Wave + Local Orbitals Program for Calculating Crystal Properties (Karlheinz Schwarz, Techn. Universität Wien, Austria), 2001. ISBN 3-9501031-1-2.

⁷ K. Mackay, J. Nucl. Mater. **8**, 263, (1963).

⁸ T. Hahn, ed., *International Tables for Crystallography*, Kluwer Academic Publishers, Dordrecht, The Netherlands, (2002).

⁹ M. G. Ganchenkova, P. V. Vladimirov, and V. A. Borodin, J. Nucl. Mater. **386**, 79 (2009).

¹⁰ P. Zhang, J. Zhao, B. Wen, J. Phys.: Condens. Matter **24**, 095004, (2012).

¹¹ P. Zhang, J. Zhao, B. Wen, J. Nucl. Mater. **423**, 164, (2012).

¹² J. Cayphas, J. Nucl. Mater. **246**, 171 (1997).

¹³ M. Sanati and S. K. Estreicher, Solid State Commun. **128**, 181, (2003).

¹⁴ J. P. Perdew and Y. Wang, Phys. Rev. B **45**, 13244, (1992).

¹⁵ K. Burke, J. P. Perdew, and Y. Wang, in *Electronic density functional theory: recent progress and new directions*, edited by J. Dobson, G. Vignale, and M. Das (Plenum Press, 1998).

¹⁶ G. Kresse and J. Hafner, Phys. Rev. B **47**, 558, (1993).

¹⁷ G. Kresse and J. Furthmüller, Phys. Rev. B **54**, 11169, (1996).